Polymer Chemistry

COMMUNICATION

View Article Online
View Journal | View Issue

Cite this: *Polym. Chem.*, 2017, **8**, 2909

Received 9th February 2017,
Accepted 23rd April 2017

DOI: 10.1039/c7py00226b

rsc.li/polymers

ATRP mediated encapsulation of Gibbsite: fixation of the morphology by using a cross-linker†

Olessya P. Loiko,[a] Anne B. Spoelstra,[a] Alexander M. van Herk,[a,b] Jan Meuldijk[a] and Johan P. A. Heuts *[a]

Using ethylene glycol dimethacrylate (EGDMA) as a cross-linker Gibbsite platelets were successfully encapsulated fully using an ATRP-mediated emulsion polymerisation technique. Previously we reported a "muffin-like" morphology, which was obtained using the same approach without a cross-linker. This morphology was attributed to the mobility of the growing polymeric chains, allowing them to move one side of the platelet during the reaction. The addition of EGDMA reduces this mobility and it is shown that this approach indeed leads to encapsulated Gibbsite. A comprehensive study of the reaction conditions, in particular the cross-linker addition profile and concentration, was carried out in combination with cryo-TEM characterization of the final particle morphology.

Polymer encapsulation of single clay platelets is one of the most challenging aspects in the field of polymer–clay nanocomposites.[1–3] Common encapsulation techniques usually involve surface-initiated polymerisation where immobilisation of an initiator on the surface *via* chemical attachment is required.[4,5] Alternative routes mainly lead to the so-called armored,[6–8] peanut-shaped,[9] dumbbell[10,11] and muffin-like[12] morphologies. Only a few studies reported the successful encapsulation of clay platelets.[13–15] Therefore, encapsulation of clay still remains challenging.

Our group previously reported the successful encapsulation of Gibbsite platelets using a strategy based on reversible addition–fragmentation chain transfer (RAFT) in a starved feed emulsion polymerisation.[16] Briefly, a random anionic co-oligomer, consisting of butyl acrylate (BA) and acrylic acid (AA) units, was synthesised using RAFT polymerization. These co-oligomers were then adsorbed onto the surface of Gibbsite platelets and subsequently chain extended by the addition of an initiator and feeding of a hydrophobic monomer mixture. Recently we extended this approach to ATRP, in which similar anionic co-oligomers were used, but now synthesized using ATRP and thus containing a bromine functionality instead of a RAFT functionality (Scheme 1).[12] In the subsequent (Cu-mediated) starved-feed emulsion polymerization, these adsorbed chains now acted as macro-initiators rather than as reversible chain transfer agents as in the case of the RAFT-based approach. Since these co-oligomers also act as stabilizers of the initial Gibbsite and resulting polymer dispersion, no additional surfactant was required in this approach. Cryo-TEM characterisation revealed a "muffin-like" morphology of the obtained hybrid latex particles and not the truly encapsulated Gibbsite platelets as were obtained in the RAFT-based approach. This morphology was not affected by the monomer feeding profile or composition. It is conceivable that the obtained morphology was caused by a high mobility of the adsorbed ATRP macroinitiator and growing chains on the surface of the platelets, leading to polymerisation on only a single face of the platelet, and that the addition of a cross-linker would reduce this mobility. A similar approach was reported by Matyjaszewski and co-workers for the encapsulation of gold nanoparticles[17] and organic dyes.[18] In the present work, we investigated the addition of the cross-linker ethylene glycol dimethacrylate (EGDMA) as a new element in the previously published ATRP-based approach.

Cryo-TEM was used to study the morphology of the synthesised nanocomposites. Parameters such as the amount and addition profile of EGDMA were investigated with a focus on the resulting particle morphology and colloidal stability.

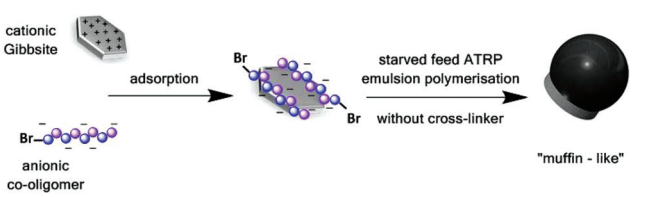

Scheme 1 Schematic illustration of ATRP-based synthesis of polymer–Gibbsite nanocomposites using an anionic co-oligomer as a stabiliser and macroinitiator.

[a]*Department of Chemical Engineering and Chemistry, Eindhoven University of Technology, PO Box 513, 5600 MB Eindhoven, The Netherlands. E-mail: j.p.a.heuts@tue.nl*
[b]*Institute of Chemical and Engineering Sciences, 1 Pesek Road, Jurong Island 627833, Singapore*

†Electronic supplementary information (ESI) available: Experimental and characterisation details. See DOI: 10.1039/c7py00226b

Effect of EGDMA addition

Previously reported encapsulation experiments used a starved-feed addition of a methyl methacrylate (MMA)/butyl acrylate (BA) monomer mixture to the Gibbsite dispersion as a prerequisite for efficient encapsulation.[12,13,19] Since it was not *a priori* clear how and when the cross-linker has to be added in the process, we investigated three different addition profiles of EGDMA (10 wt% based on overall monomer content), while maintaining the previously[12] employed MMA/BA feeding profile (Fig. 1a).

As can be seen from Fig. 1a, in profile I the total amount of EGDMA was injected into the reaction mixture as a single shot and reacted for two hours. After this two hours reaction of EGDMA, the MMA/BA monomer addition was started. In profile II the same amount of EGDMA was fed over a period of about 1 h prior to the monomer addition. Finally, in profile III both the cross-linker and the monomer mixture were mixed and fed to the reactor. In all cases, the initial ATRP macroinitiator–Gibbsite dispersion was characterized to have $D_z \approx$ 100 nm (poly ≈ 0.14) and ζ-potential ≈ −50 mV. The effect of the EGDMA addition profile on the colloidal stability of the nanocomposites during the reaction was studied by measuring D_z (Fig. 1b) and the ζ-potential (see the ESI†). As expected, the results presented in Fig. 1b clearly show an increase in particle size during all three reactions. However, the very large diameters ($D_z \approx$ 1000 nm, with poly ≈ 1) of the particles in the samples from profile I suggested the formation of colloidally unstable latex particles, which was confirmed by TEM imaging of the final latex (Fig. 2a). Profiles II and III resulted in colloidally stable dispersions with $D_z \approx$ 240 nm (poly ≈ 0.15) and $D_z \approx$ 215 nm (poly ≈ 0.17), respectively. TEM images of the products resulting from these two feeding profiles are shown in Fig. 2b and c, respectively.

The cryo-TEM image (Fig. 2b) clearly shows a complete coverage of Gibbsite platelets with the polymer, when gradual feeding of the cross-linker prior to MMA/BA addition was used (profile II). In the case of simultaneously feeding the cross-linker with the other monomers (profile III) two types of morphologies ("muffin-like" and encapsulated platelets) are observed (Fig. 2c).

In order to further quantify these observations, particle counting (>100 particles) for the last two cases was conducted (Fig. 3).

These results clearly demonstrate that the predominant product (>80%) resulting from profile II is truly encapsulated Gibbsite platelets, with only a minor amount of "muffin"-structures. We therefore decided to use a cross-linker feed prior to monomer feed in our remaining studies.

Effect of EGDMA concentration

It is clear from the previous section that although slow feeding of EGDMA prior to monomer addition dramatically improved the resulting morphology with more than 80% encapsulated Gibbsite platelets, a small fraction of "muffin-like" particles

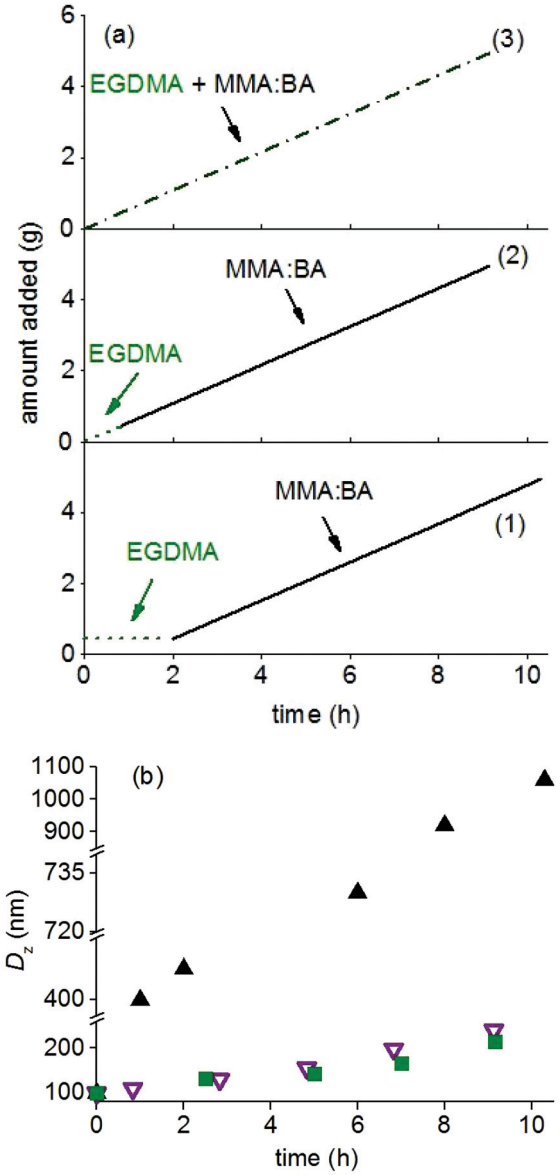

Fig. 1 (a) Addition profiles of EGDMA (dashed line) and MMA/BA (solid line), and (b) evolution of the *Z*-average particle diameter D_z obtained using these profiles: (▲) profile I, (▽) profile II and (■) profile III. Reaction conditions: V_{water} = 30 mL, T = 70 °C, 6 mg of ATRP macroinitiator and 20 mg of Gibbsite per mL, $[\text{ascorbic acid}]_0 = 2.6 \times 10^{-6}$ M, $[Cu^{2+}]_0 = 2.6 \times 10^{-6}$ M, MMA : BA = 10 : 1 w/w, feeding rates of ascorbic acid, MMA/BA and EGDMA were 9 mg min^{-1}. Final product consists of 247.5 g of polymer per g of Gibbsite.

was still present. We therefore used profile II and studied the effect of the EGDMA amount on the morphology of polymer–Gibbsite nanocomposites: 5, 10, 15 and 20 wt% based on the overall monomer content.

The evolution of the *Z*-average particle diameter and the zeta-potential in encapsulation experiments was studied. For all cross-linker contents, except for 20 wt%, the obtained results were very similar to those reported for profile II as shown in Fig. 1b; the results for 20 wt% were similar to

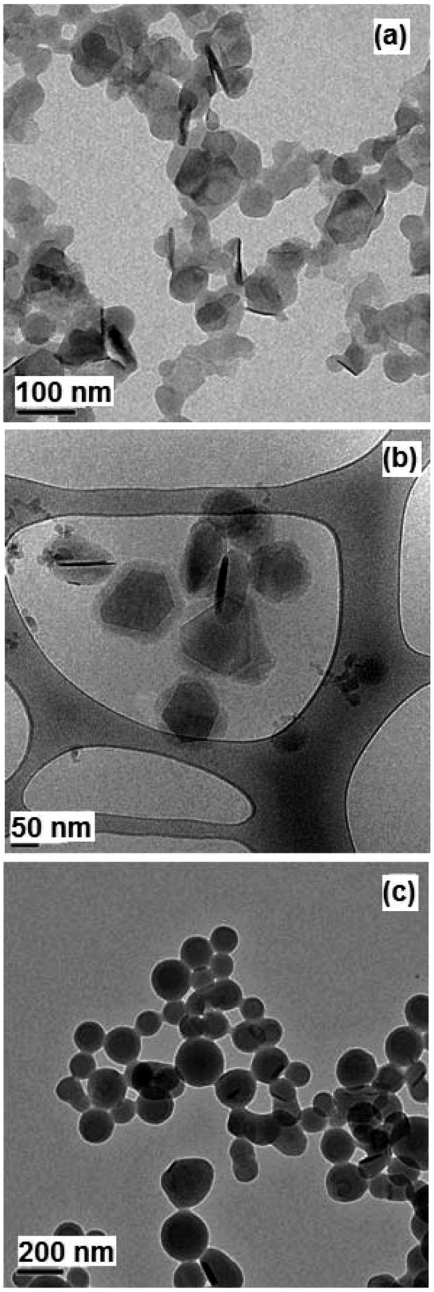

Fig. 2 TEM (a, c) and cryo-TEM (b) images of polymer–Gibbsite latex particles obtained using different addition profiles of EGDMA: (a) profile I, (b) profile II and (c) profile III. Other conditions as in Fig. 1.

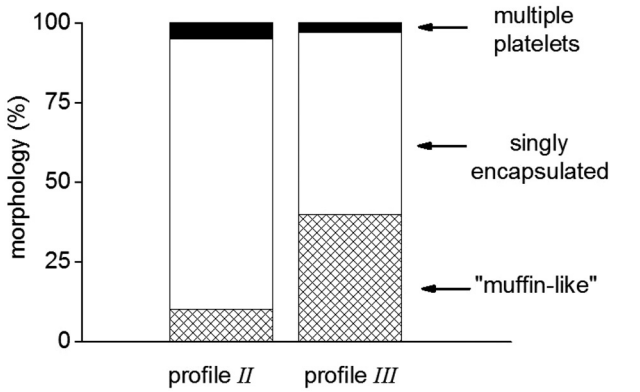

Fig. 3 Observed morphologies (%) for different EGDMA addition profiles.

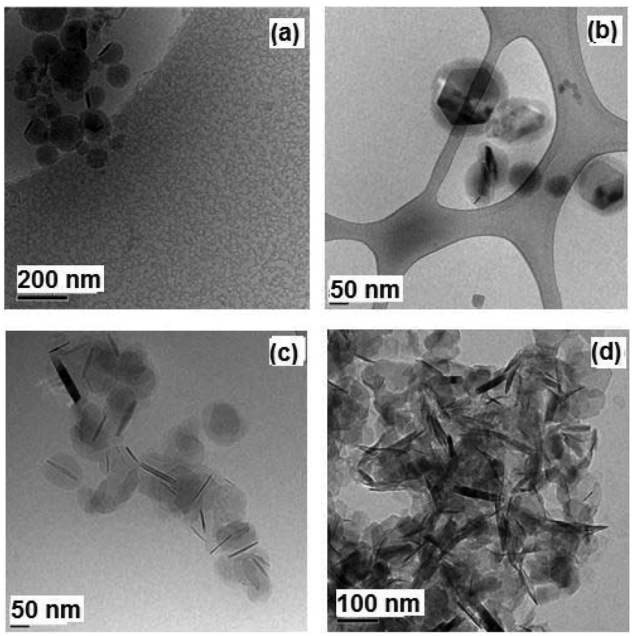

Fig. 4 cryo-TEM (a–c)/TEM (d) images of polymer–Gibbsite latex particles obtained using profile II for different EGDMA contents: (a) 5 wt%, (b) 10 wt%, (c) 15 wt% and (d) 20 wt%. Other conditions as in Fig. 1.

those shown for profile I in Fig. 1b (for more details, see the ESI†).

The morphology of the synthesised nanocomposites was studied using (cryo-)TEM and the results are shown in Fig. 4.

The results clearly show the effect of cross-linker concentration on the morphology of polymer–Gibbsite latex particles. In the case of a low EGDMA concentration (Fig. 4a) a "muffin-like" morphology was observed, similar to what was previously reported for the case without a cross-linker.[12] This suggests that the used EGDMA concentration is not sufficient to fixate the growing chains. As was discussed above encapsulated particles with a small fraction of "muffin-like" morphology were observed in the case of 10 wt% (Fig. 4b). Increasing the amount of EGDMA led to cross-linking between the platelets and growth of the polymer around these aggregates (Fig. 4c). An even more drastic effect was observed for a cross-linker content of 20 wt% (Fig. 4d). The overall result was very similar to what was observed for profile I, *i.e.*, all EGDMA added in a single shot. We can therefore conclude that the most successful encapsulation was achieved for an EGDMA content of 10 wt%.

It is clear from the results of this work, that both addition profile and concentration of EGDMA affect the morphology

and colloidal stability of the resulting polymer–Gibbsite latex particles.

The morphology of the final hybrid particles depends on kinetic and thermodynamic factors;[5] the Gibbsite normally would preferentially be in contact with the aqueous phase and the muffin structure obtained without a crosslinker could thus be regarded as an equilibrium morphology. Due to the initially low molecular weights in the (crosslinker-free) ATRP approach the mobility of the growing chains is high and the equilibrium can be achieved. The addition of a crosslinker early in the reaction limits this mobility and another type of morphology is obtained (fully encapsulated Gibbsite).

Conclusions

In the present work successfully encapsulated Gibbsite platelets were obtained using EGDMA as a cross-linker in the ATRP-mediated starved feed emulsion copolymerisation of MMA and BA. It was previously reported that using the same ATRP-based approach, but without a cross-linker led to a "muffin-like" morphology.[12] The observed difference in morphologies supports the idea of reducing the mobility of a macroinitiator and growing chains by introducing a cross-linker into the system. The effects of the cross-linker addition profile and concentration on the resulting particle morphology were studied. Cryo-TEM characterisation revealed different types of morphologies depending on these studied parameters and that the best results were obtained by slowly feeding the cross-linker (10 wt% with respect to overall monomer content) prior to the start of the MMA/BA feeding.

Acknowledgements

The authors thank Stefan Bon for valuable discussions and the Euro-Asian Cooperation for Excellence and Advancement, Stichting Emulsion Polymerisation and A*STAR Research Attachment Programme for financial support.

Notes and references

1 E. Zengeni, P. Hartmann and H. Pasch, *ACS Appl. Mater. Interfaces*, 2012, **4**, 6957–6968.
2 B. zu Putlitz, K. Landfester, H. Fischer and M. Antonietti, *Adv. Mater.*, 2001, **13**, 500–503.
3 S. Cauvin, P. J. Colver and S. A. F. Bon, *Macromolecules*, 2005, **38**, 7887–7889.
4 L. B. de Paiva, A. R. Morales and F. R. V. Diaz, *Appl. Clay Sci.*, 2008, **42**, 8–24.
5 A. M. van Herk, *Macromol. React. Eng.*, 2015, **10**, 22–28.
6 T. R. Guimarães, T. C. Chaparro, F. D'Agosto, M. Lansalot, A. M. D. Santos and E. Bourgeat-Lami, *Polym. Chem.*, 2014, **5**, 6611–6622.
7 N. Negrete-Herrera, J.-M. Letoffe, J.-L. Putaux, L. David and E. Bourgeat-Lami, *Langmuir*, 2004, **20**, 1564–1571.
8 N. Negrete-Herrera, J.-L. Putaux, L. David, F. De Haas and E. Bourgeat-Lami, *Macromol. Rapid Commun.*, 2007, **28**, 1567–1573.
9 D. J. Voorn, W. Ming and A. M. van Herk, *Macromol. Symp.*, 2006, **245–246**, 584–590.
10 D. J. Voorn, W. Ming and A. M. van Herk, *Macromolecules*, 2006, **39**, 4654–4656.
11 A. Bonnefond, M. Mičušík, M. Paulis, J. R. Leiza, R. F. A. Teixeira and S. A. F. Bon, *Colloid Polym. Sci.*, 2013, **291**, 167–180.
12 O. P. Loiko, A. B. Spoelstra, A. M. van Herk, J. Meuldijk and J. P. A. Heuts, *Polym. Chem.*, 2016, **7**, 3383–3391.
13 O. P. Loiko, A. B. Spoelstra, A. M. van Herk, J. Meuldijk and J. P. A. Heuts, *RSC Adv.*, 2016, **6**, 80748–80755.
14 Y. Reyes, P. J. Peruzzo, M. Fernandez, M. Paulis and J. R. Leiza, *Langmuir*, 2013, **29**, 9849–9856.
15 M. A. Mballa Mballa, J. P. A. Heuts and A. M. van Herk, *Colloid Polym. Sci.*, 2012, **291**, 501–513.
16 S. I. Ali, J. P. A. Heuts, B. S. Hawkett and A. M. van Herk, *Langmuir*, 2009, **25**, 10523–10533.
17 H. Dong, M. Zhu, J. A. Yoon, H. Gao, R. Jin and K. Matyjaszewski, *J. Am. Chem. Soc.*, 2008, **130**, 12852–12853.
18 W. Li and K. Matyjaszewski, *Polym. Prepr.*, 2011, **52**, 89–90.
19 W.-D. Hergeth, P. Starre, K. Schmutzler and S. Wartewig, *Polymer*, 1988, **29**, 1323–1328.

